Journal of Ginseng Research 48 (2024) 31–39

Contents lists available at ScienceDirect

Journal of Ginseng Research

journal homepage: www.sciencedirect.com/journal/journal-of-ginseng-research

Research Article

Rg3-enriched red ginseng extracts enhance apoptosis in $CoCl_2$-stimulated breast cancer cells by suppressing autophagy

Yun-Jeong Jeong [a, 1], Mi-Hee Yu [a, 1], Yuna Cho [a], Min-Young Jo [a], Kwon-Ho Song [a], Yung Hyun Choi [b], Taeg Kyu Kwon [c], Jong-Young Kwak [d, **], Young-Chae Chang [a, *]

[a] Research Institute of Biomedical Engineering and Department of cell Biology, Catholic University of Daegu School of Medicine, Daegu, Republic of Korea
[b] Department of Biochemistry, College of Korean Medicine, Dong-Eui University, Busan, Republic of Korea
[c] Department of Immunology, School of Medicine, Keimyung University, Daegu, Republic of Korea
[d] Department of Pharmacology, School of Medicine, Ajou University, Suwon, Republic of Korea

ARTICLE INFO

Article history:
Received 14 December 2022
Received in revised form
5 June 2023
Accepted 6 June 2023
Available online 7 June 2023

Keywords:
Rg3-enriched red ginseng extracts
autophagy
apoptosis
ROS

ABSTRACT

Background: Ginsenoside Rg3, a primary bioactive component of red ginseng, has anti-cancer effects. However, the effects of Rg3-enriched ginseng extract (Rg3RGE) on apoptosis and autophagy in breast cancer have not yet been investigated. In the present study, we explored the anti-tumor effects of Rg3RGE on breast cancer cells stimulated $CoCl_2$, a mimetic of the chronic hypoxic response, and determined the operative mechanisms of action.
Methods: The inhibitory mechanisms of Rg3RGE on breast cancer cells, such as apoptosis, autophagy and ROS levels, were detected both *in vitro*. To determine the anti-cancer effects of Rg3RGE *in vivo*, the cancer xenograft model was used.
Results: Rg3RGE suppressed $CoCl_2$-induced spheroid formation and cell viability in 3D culture of breast cancer cells. Rg3RGE promoted apoptosis by increasing cleaved caspase 3 and cleaved PARP and decreasing Bcl2 under the hypoxia mimetic conditions. Further, we identified that Rg3RGE promoted apoptosis by inhibiting lysosomal degradation of autophagosome contents in $CoCl_2$-induced autophagy. We further identified that Rg3RGE-induced apoptotic cell death and autophagy inhibition was mediated by increased intracellular ROS levels. Similarly, in the *in vivo* xenograft model, Rg3RGE induced apoptosis and inhibited cell proliferation and autophagy.
Conclusion: Rg3RGE-stimulated ROS production promotes apoptosis and inhibits protective autophagy under hypoxic conditions. Autophagosome accumulation is critical to the apoptotic effects of Rg3RGE. The *in vivo* findings also demonstrate that Rg3RGE inhibits breast cancer cell growth, suggesting that Rg3RGE has potential as potential as a putative breast cancer therapeutic.

1. Introduction

Breast cancer is the most diagnosed cancer in women worldwide and in Korea [1]. Presently, multiple treatment modalities are employed for breast cancer, such as surgical resection, radiation therapy, and chemotherapy [2]. Although these treatments significantly improve breast cancer survival rate, the quality of life for breast cancer patients undergoing standard chemotherapy is poor [3]. Therefore, the development of new effective therapeutic strategies is important for the treatment of breast cancer.

Apoptosis, a form of type I programmed cell death (PCD), is a cell death pathway characterized by caspase activation and DNA fragmentation [4]. Type II PCD exhibits morphological characteristics of autophagy, which is a lysosome-dependent process involving

Abbreviations: Rg3RGE, Rg3-enriched ginseng extract; PCD, Programmed cell death; 3D cells, Three-dimensional cells; LC3, Light chain 3A/B; DMSO, Dimethyl sulfoxide; DMEM, Dulbecco's modified eagle medium; WST-8, Water-soluble tetrazolium 8; RIPA, Radioimmunoprecipitation assay; SDS-PAGE, Sodium dodecyl-sulfate polyacrylamide gel electrophoresis; PBS, Phosphate-buffered saline; DAPI, 4′,6-Diamidino-2-Phenylindole; DCF-DA, 2′,7′-Dichlorofluorescein diacetate; IHC, Immunohistochemistry; CQ, Chloroquine; HIF-1α, Hypoxia inducible factor-1α; ROS, Reactive oxygen species; NAC, N-acetyl-L-cysteine; RGE, Red ginseng extract.

* Corresponding author. Research Institute of Biomedical Engineering and Department of cell Biology, Catholic University of Daegu School of Medicine, Daegu, 42472, Republic of Korea.
** Corresponding author. Department of Pharmacology, School of Medicine, Ajou University, Suwon, 16499, Republic of Korea.
E-mail addresses: jykwak@ajou.ac.kr (J.-Y. Kwak), ycchang@cu.ac.kr (Y.-C. Chang).
[1] These authors have contributed equally to this paper.

https://doi.org/10.1016/j.jgr.2023.06.001

formation of autophagosomes containing damaged cytoplasmic components and their subsequent lysosomal degradation [5]. Contrastingly, autophagy is also a homeostatic regulator that can suppress apoptosis [6]. Inhibition of autophagy by disruption of autophagic flux results in aberrant autophagosome accumulation, promoting cell death [7]. Apoptosis and autophagy are activated by adverse intracellular environments such as starvation, growth factor deficiency, and hypoxia [8]. Hypoxia induced by uncontrolled tumor growth and deficient tumor vascularity increases autophagy, promoting cell survival under starvation conditions [9]. Therefore, controlling the balance between apoptosis and autophagy is an important target for cancer treatment under hypoxic conditions.

Korean Red Ginseng is a traditional medicine manufactured by steaming and drying raw ginseng and is used to treat inflammatory and cardiovascular diseases [10,11]. The primary bioactive component of red ginseng, Ginsenoside Rg3, and Rg3-enriched ginseng extract (Rg3RGE) have anti-cancer effects [12,13]. In multiple cancer cell types, including breast, prostate, and lung cancer cells, Rg3 inhibition of cancer growth is mediated by suppressing NF-κB signaling [14–16]. In addition, the apoptotic activity of Rg3 in Hela cells is mediated by inhibition of starvation-induced autophagic flux [17]. Despite robust evidence for the anti-cancer effects of Rg3-mediated apoptosis and autophagy, the effects of Rg3RGE on apoptosis and autophagy in breast cancer and the underlying mechanisms of action have not been investigated.

In the present study, we investigated the anti-cancer effects of Rg3RGE in breast cancer cells by determining its regulatory effects on the balance between apoptosis and autophagy. We identified that under hypoxic conditions, Rg3RGE inhibits cell proliferation and spheroid formation and induces apoptosis by disrupting autophagy. This is the first report that Rg3RGE is a potential breast cancer therapeutic and identifies a novel mechanism of action mediated by increased reactive oxygen species (ROS) levels and subsequent regulation of apoptosis and autophagy *in vitro* and *in vivo*.

2. Materials and methods

2.1. Materials and cells culture

Rg3RGE was supplied by Korea Ginseng corporation (Daejeon, Gimhae-si, Korea). Rg3RGE contained enriched ginsenoside-Rg3 as determined by performance liquid chromatography (Korea Ginseng Corporation) (Table 1) [18]. Rg3RGE was dissolved in 50% dimethyl sulfoxide (DMSO), stored at −20°C, and diluted in medium before use. MCF-7 and MDA-MB-231 breast cancer cells were obtained from the American Type Culture Collection (Manassas, VA, USA). Cells were incubated in Dulbecco's modified eagle medium (DMEM) (HyClone; GE Healthcare Life Sciences, Logan, UT, USA) containing 10% fetal bovine serum (HyClone) and 1% antibiotic mixture in an atmosphere containing 5% CO_2 at 37°C. Densitometric analysis of scanned images was performed using the ImageJ software (version 2018; National Institutes of Health, Bethesda, MD, USA).

Table1
Ginsenoside contents of Rg3-enriched ginseng extract.

ginsenosides	Contents (mg/g)
Total ginsenosides	67.41
20(S)-Rg3	44.91
20(R)-Rg3	6.78
Rb1	3.86
Rc	1.20
Rb2	1.53
Rd	1.60
Rf	1.28
Rh1	3.71
20(S)-Rg2	3.55

2.2. Three-dimensional cell culture

5×10^4 breast cancer cells were seeded onto Three-dimensional (3D) nanofiber/8-well plate (Nanofaentech, Korea). After three days, cells were incubated with medium containing $CoCl_2$ or Rg3RGE for 24 h. Cell morphology and immunofluorescence were measured as follows.

2.3. Cell viability assay

The breast cancer cells were seeded onto the nanofiber/8-well plate at 5×10^4 and incubated. After three days, cells were incubated with medium containing $CoCl_2$ or Rg3RGE for 24 h, and then treated with water-soluble tetrazolium 8 (WST-8) reagent (Biomax Co. Seoul, South Korea) for 2 h. Absorbance was measured at 450 nm on a spectrophotometer.

2.4. Trypan blue stanning assay

2×10^5 cells were seeded in 6-well plates and replaced with fresh medium containing with $CoCl_2$ and Rg3RGE and incubated for 24 days. The cells were staining with trypan blue. The percentage of death cell were analyzed by the number of trypan blue positive cells.

2.5. Colony formation assay

1×10^4 cells were seeded in 6-well plates and incubated for 5 days. Cells were replaced with fresh medium containing $CoCl_2$ and Rg3RGE and incubated for 48 h. The cells were fixed with 100 % methanol and stained with 0.5% crystal violet for 1 h.

2.6. Western blot analysis

After indicated drugs treatment for 24 h, the cells were extracted in radioimmunoprecipitation assay (RIPA) lysis buffer. Equal amounts of lysates sample were subjected to sodium dodecyl-sulfate polyacrylamide gel electrophoresis (SDS-PAGE) and transferred to an Immobilon-P-membrane (Millipore, USA). After incubation of the membranes with primary antibody at 4°C overnight, the membranes were washed three times with TBS-T and incubated with secondary antibodies for 1 h at room temperature. Signals were detected by chemiluminescence (GE Healthcare, Chicago, IL, USA) on a ChemiDOC™ XRS (Bio-Rad Laboratories, Hercules, CA, USA).

2.7. PI/Annexin V stanning and flow cytometry assay

After indicated drugs treatment for 24 h, cells were washed twice with phosphate-buffered saline (PBS). Cells were suspended in 200 μl binding buffer, to which were added PI and Annexin V-FITC for 30 min at 4 °C in dark room (BD Biosciences, San Jose, CA, USA). Fluorescence was assessed for cell apoptosis by flow cytometry (Beckman Coulter, CA, USA).

2.8. Immunofluorescence assay

Cells were seeded onto nanofiber/8-well plate and 8 well slid glass. Cells were incubated with the indicated drugs for 24 h, and then were incubated lysotracker-red (Thermo Fisher Scientific). Cells were fixed in 100% methanol, and were blocked with 10% normal goat serum. Cells were further incubated with primary

antibodies against light chain 3A/B (LC3) antibody for overnight at 4°C. Cells were washed with PBS three times, and reacted with FITC-conjugated anti-rabbit secondary antibodies and stained with 4′,6-diamidino-2-Phenylindole (DAPI) for 5 min. Fluorescence was detected by confocal microscopy (Leica Microsystems GmbH, Wetzlar, Germany).

2.9. ROS activity

Cells were incubated with the indicated drugs for 24 h, followed by further incubation with 10 μM 2′,7′-dichlorofluorescein diacetate (DCF-DA) for 1 h. Fluorescence was detected in equivalent quantities of protein on a SpectraMax® iD5 multi-plate reader (Molecular devices, shanghai, China; excitation:530 nm, emission: 485 nm)

2.10. Tumor xenograft model

BALB/c nude mice (Female, 6 weeks old) were purchased from Lab Animal (Seoul, Korea) and maintained in pathogen-free conditions. The mice were inoculated with 2×10^7 MCF-7 cells subcutaneously in the right flank. After the formation of palpable

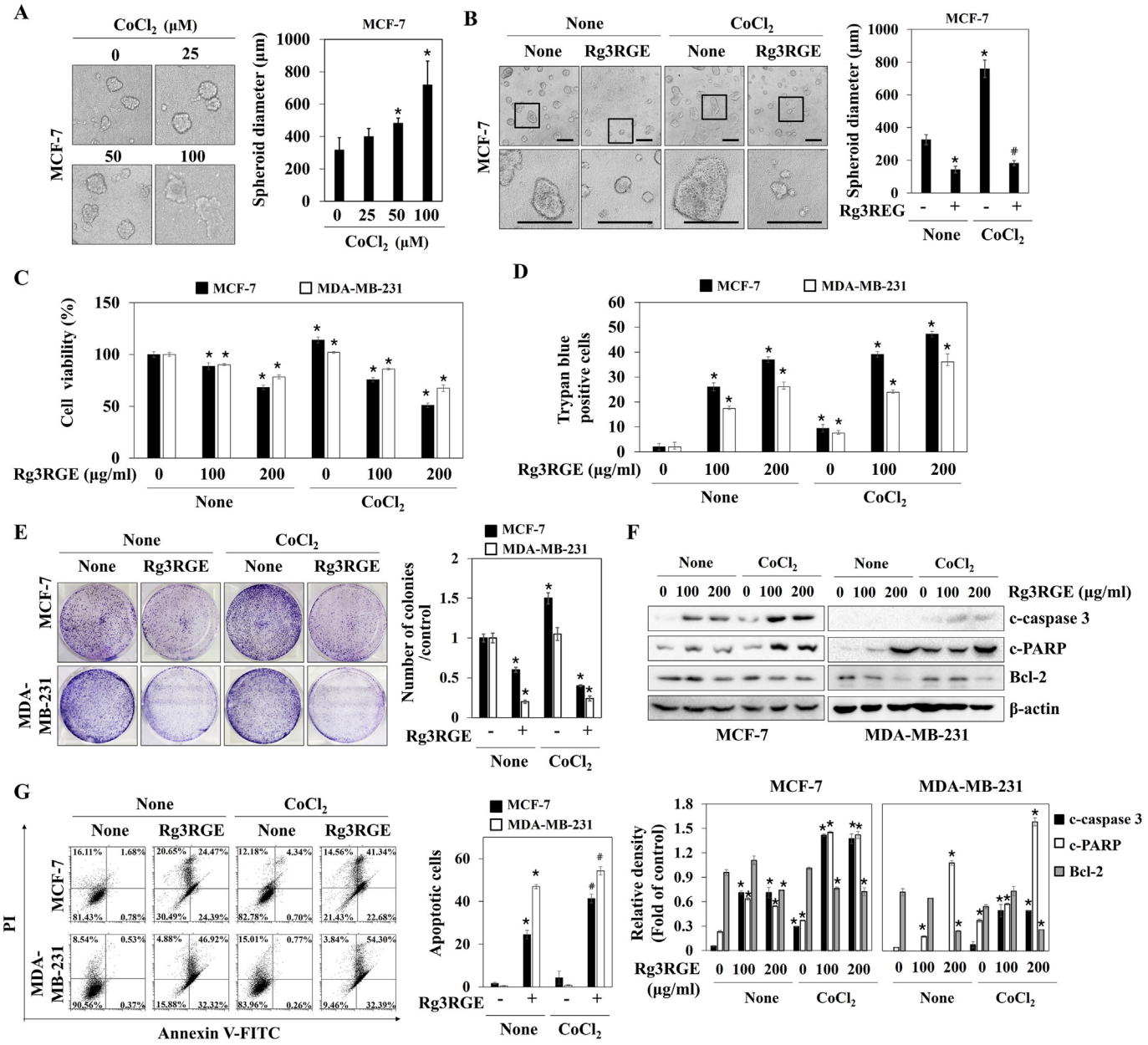

Fig. 1. Rg3RGE inhibits cell proliferation and promotes apoptosis in $CoCl_2$-stimulated breast cancer cells. (A and B) MCF-7 cells were seeded onto 3D nanofiber/8-well plate for 3D cells. Three-dimensional (3D) cells were cultured with medium containing $CoCl_2$ (25, 50, and 100 μM) and Rg3RGE (200 μg/ml) for 24 h, and then photographed. (C) The 3D cultured cells were treated with $CoCl_2$ (100 μM) or Rg3RGE (200 μg/ml) for 24 h, followed by treatment with WST-1 solution for 2 h. (D) The number of trypan blue stained cells in the 3D culture was analyzed. (E) Proliferation rate was analyzed by colony formation assay. Cell colonies were detected by crystal violet staining and counted. (F) Cells were treated with the indicated drugs for 24 h. The levels of cleaved-caspase3 and cleaved-PARP, and Bcl2 were determined using western blot assay. β-actin was used as a loading control. (G) Rates of apoptosis in breast cancer cells treated with $CoCl_2$ (100 μM) Rg3RGE (200 μg/ml) for 24 h were detected by flow cytometry. The protein levels were quantified using ImageJ. Results represent mean ± S.E.M. of three independent experiments. $^*P < 0.05$ vs. control. $^{\#}P < 0.05$ vs. Rg3RGE.

tumors (~5 mm), the mice were randomized into five condition groups (n = 5/group). Next, the mice were treated with 50 mg/kg/100 μl (PBS containing 0.05% (v/v) Tween 20) Rg3RGE once every two days. The mice were euthanized on day 21 after which tumor weights were determined. Animal care and all experimental procedures were approved by and conducted in accordance with the guidelines of the Institutional Animal Care and Use Committee of the Catholic University of Daegu.

2.11. Immunohistochemistry (IHC)

The paraffin-embedded mouse tumor sections were mounted on microscope slides. The tissue sections were maintained with primary antibodies at 4°C overnight. Secondary antibodies were incubated at 37°C for 30 min. 3,3′-diaminobenzidine tetrahydrochloride was used as the coloring reagent, and hematoxylin was used as the counterstain. Tumor sections were observed using a Pannoramic MIDI slide scanner (3DHISTECH, Budapest, Hungary).

2.12. Statistical analysis

All *in vitro* and *in vivo* results presented were derived from at least three independent experiments performed in triplicate. Results were analyzed using Graph Pad Prism 5 software (Graph Pad Software, La Jolla, CA, USA). The one-way ANOVA followed by Bonferroni post hoc test was used to determine the significance of differences between experimental and control values. *P*–values of < 0.05 were taken to indicate significant differences.

3. Results

3.1. Rg3RGE inhibits spheroid formation and induces apoptosis in $CoCl_2$-stimulated breast cancer cells

$CoCl_2$, which suppresses PHD2 activation, is commonly used to mimic hypoxia. To investigate the potential anti-cancer effects of Rg3RGE in breast cancer cells in a hypoxic microenvironment, we determined the effects of $CoCl_2$ and Rg3RGE on spheroid formation using 3D culture. 100 μM $CoCl_2$ increased MCF-7 cell spheroid diameter 2-fold relative to control, so this concentration was used in subsequent experiments (Fig. 1A). Rg3RGE (200 μg/ml) significantly inhibited spheroid formation in both the presence and absence of $CoCl_2$ (Fig. 1B). Result of WST assay in the 3D culture model revealed that Rg3RGE significantly decreased cell viability, and that this effect was more pronounced in hypoxia-like conditions relative to normal conditions (Fig. 1C). Similarly, the number

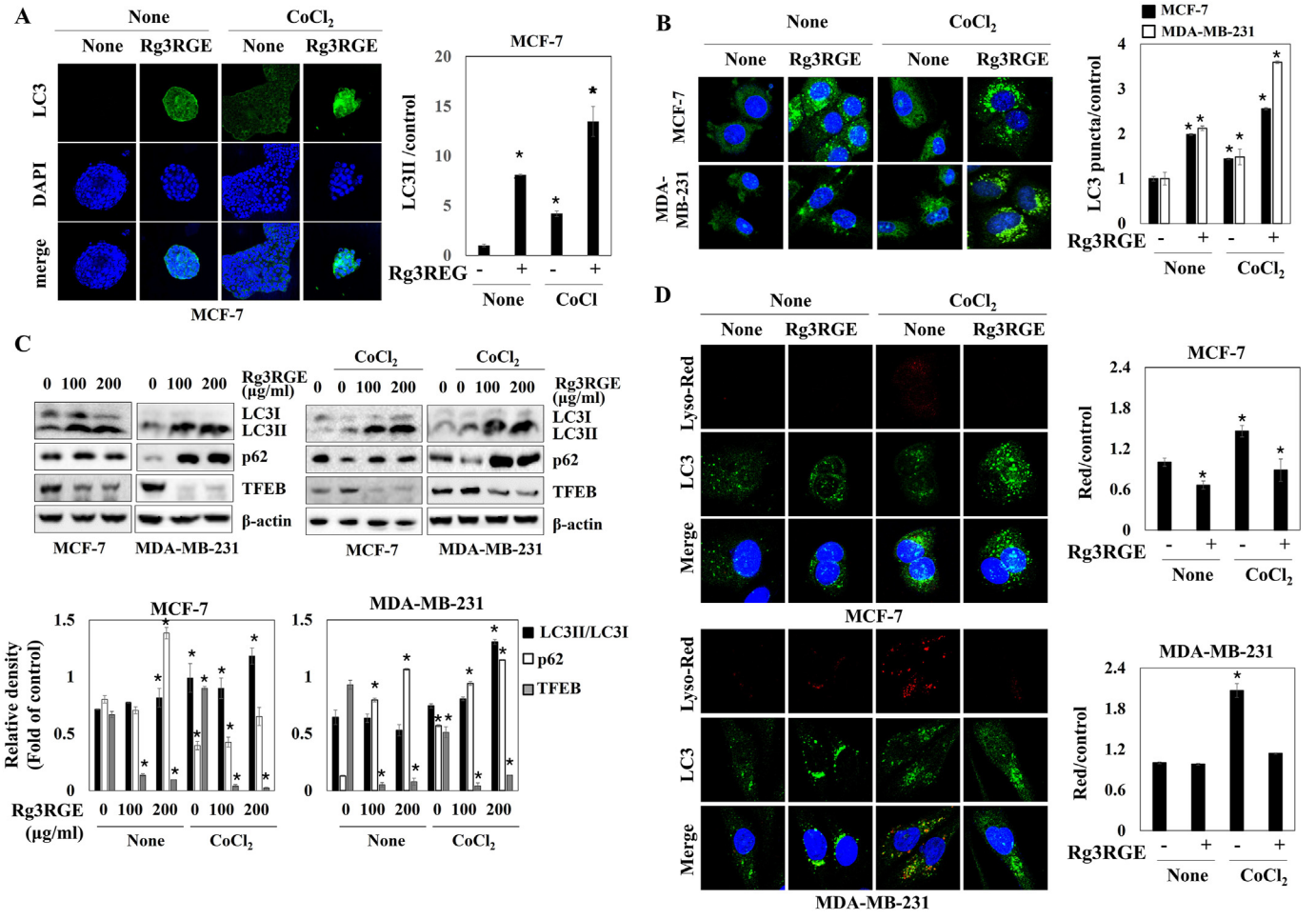

Fig. 2. Rg3RGE inhibits $CoCl_2$-induced autophagy in breast cancer cells. (A and B) Indicated cells were seeded onto 3D nanofiber/8-well plate or in 8-well slide glass. Media was replaced with 100 μM $CoCl_2$ and 200 μg/ml Rg3RGE for 24 h, followed by incubation with antibodies against LC3. The nuclear DNA was stained with DAPI. (C) MCF-7 and MDA-MB231 cells were treated with 100 μM $CoCl_2$ and 200 μg/ml Rg3RGE for 24 h, and levels of LC3, p62, and TFEB were measured by western blotting. (D) Cells were seeded onto 8-well slide glass. Media was replaced with 100 μM $CoCl_2$ and 200 μg/ml Rg3RGE for 24 h, followed by incubation with lysotracker-red and antibodies against LC3A/B. The nuclear DNA was stained with DAPI. Densitometric analysis of LC3 levels (green fluorescence), protein levels, and red puncta levels were quantified using ImageJ. Values represent the mean ± S.E.M. of three independent experiments. *$P < 0.05$ vs. control.

of dead cells was increased by Rg3RGE under the mimic hypoxia condition in 3D culture (Fig. 1D), strongly supporting the finding that Rg3RGE suppressed $CoCl_2$-induced spheroid formation and cell viability in 3D culture.

A colony formation assay in two-dimensional culture also demonstrated that Rg3RGE decreased $CoCl_2$-induced colony formation (Fig. 1E). Furthermore, Rg3RGE more significantly increased cleaved-caspase3 and cleaved-PARP, and decreased Bcl2 under hypoxia-like conditions relative to normal conditions (Fig. 1F). Consistently, co-treatment with Rg3RGE and $CoCl_2$ markedly increased apoptotic breast cancer cells (Fig. 1G). These results strongly support that Rg3RGE promotes apoptosis in $CoCl_2$-stimulated breast cancer cells.

3.2. Rg3RGE inhibits $CoCl_2$-stimulated autophagy in breast cancer cells

Cancer cells undergo autophagy to suppress apoptosis in hypoxic environments [19]. In 3D culture, Rg3RGE not only increased LC3 expression in normoxic conditions, but also upregulated LC3 in $CoCl_2$-stimulated hypoxia-like conditions (Fig. 2A). In 2D culture, treatment with Rg3RGE or $CoCl_2$ also increased LC3 puncta. Rg3RGE significantly enhanced $CoCl_2$-induced LC3 puncta (Fig. 2B). In addition, Rg3RGE increased the protein expression of LC3, an autophagosome membrane component, as well as p62, which is degraded by formation of autolysosome, in breast cancer cells [20]. Expression of TFEB, which regulates autophagic flux by activating lysosomal biogenesis [21], was also decreased by Rg3RGE treatment. However, $CoCl_2$ promoted autophagy, increasing LC3II and TFEB expression and decreasing p62 expression. Interestingly, Rg3RGE reversed $CoCl_2$-induced upregulation of TFEB and downregulation of p62, suggesting that Rg3RGE suppressed autophagosome degradation (Fig. 2C). Accumulation of autophagosomes occurs due to suppressed autophagosome degradation, disrupting fusion of autophagosomes with lysosomes. Consistent with our hypothesis, $CoCl_2$ increased lysosome activity and colocalization of lysosome and LC3 puncta. However, Rg3RGE blocked the $CoCl_2$-induced lysosome activity (Fig. 2D), indicating that Rg3RGE suppressed autolysosome formation.

3.3. Rg3RGE enhances apoptosis by disrupting $CoCl_2$-stimulated autophagy

To determine if Rg3RGE inhibition of $CoCl_2$-induced autophagy was related to apoptosis, Rg3RGE and multiple regulators of autophagy were treated in $CoCl_2$-stimulated cells. First, rapamycin, which initiates autophagy by inhibiting mTOR did not significantly affect expression of $CoCl_2$-regulated LC3II, p62, or cleaved PARP

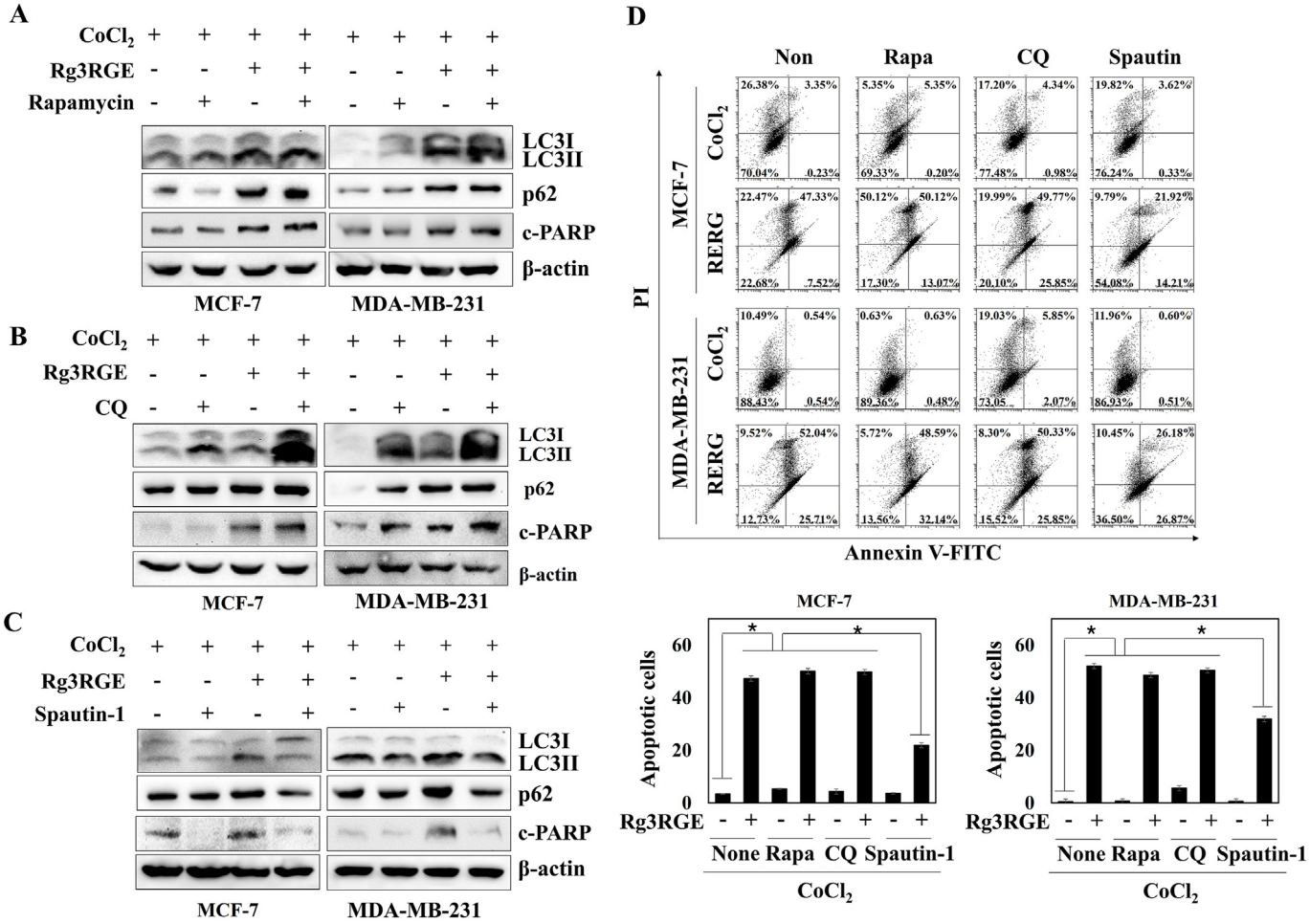

Fig. 3. Rg3RGE-induced apoptosis is associated with inhibition of autophagy. (A, B, and C) MCF-7 and MDA-MB-231 cells were treated with indicated drugs (100 μM $CoCl_2$, 200 μg/ml Rg3RGE, 500 nM rapamycin, 50 μM chloroquine, or 10 μM spautin-1) for 24 h. Levels of LC3, p62, and cleaved PARP were measured by western blotting. β-actin was used as loading control. (D) Rates of apoptosis in breast cancer cells treated with the indicated drugs (100 μM $CoCl_2$, 200 μg/ml Rg3RGE, 500 nM rapamycin, 50 μM chloroquine, or 10 μM spautin-1) for 24 h were detected by flow cytometry. Results represent mean ± S.E.M. of three independent experiments. *$P < 0.05$ vs. control.

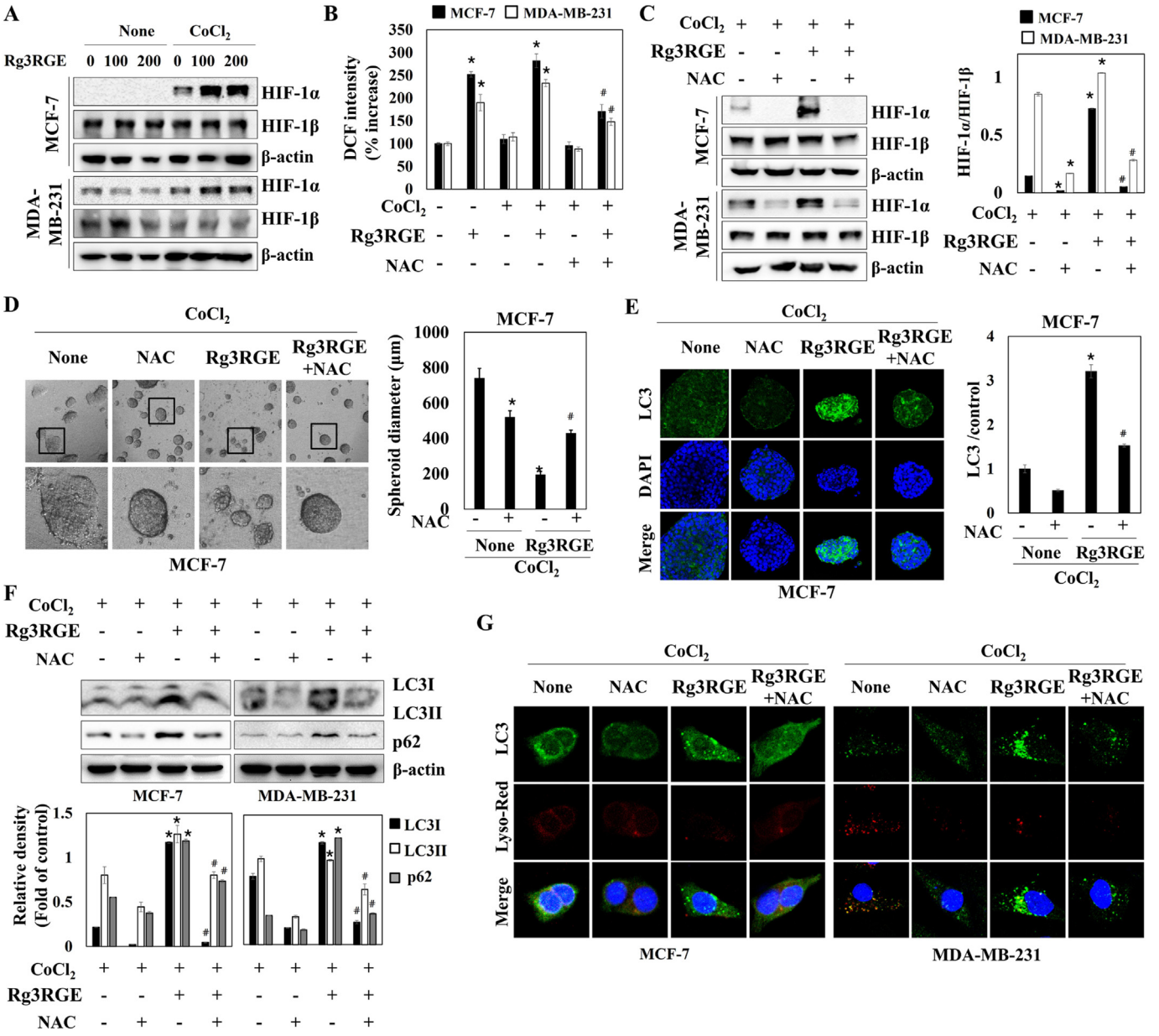

Fig. 4. Rg3RGE inhibits autophagy by increasing ROS levels. (A) MCF-7 and MDA-MB-231 cells were treated with 100 μM $CoCl_2$ and indicated concentration of Rg3RGE for 6 h, and then protein levels of HIF-1α and HIF-1β were measured by western blotting. (B) Cells were treated with 100 μM $CoCl_2$, 200 μg/ml Rg3RGE and 5 mM NAC (a ROS scavenger) for 24 h, and ROS levels were determined using DCF-DA. (C) Cells were treated with $CoCl_2$, Rg3RGE and NAC for 6 h, and protein levels of HIF-1α and HIF-1β were determined by western blotting. (D) MCF-7 cells were seeded onto 3D nanofiber/8-well plate. 3D cells were cultured with medium containing $CoCl_2$, Rg3RGE, and NAC for 24 h, and then photographed. (E) 3D cells were cultured with $CoCl_2$, Rg3RGE, and NAC for 24h, and then incubated with antibodies against LC3. The nuclear DNA was stained with DAPI. (F) After cells were treated with $CoCl_2$, Rg3RGE, and NAC for 24 h, the levels of LC3 and p62 were determined. β-actin was used as a loading control. The protein levels were quantified using ImageJ. (G) Cells were cultured with $CoCl_2$, Rg3RGE, and NAC for 24h, and then incubated with lysotracker-red and antibodies against LC3. The nuclear DNA was stained with DAPI. Results represent mean ± S.E.M. of three independent experiments. $^{*}P < 0.05$ vs. control. $^{\#}P < 0.05$ vs. Rg3RGE.

levels in co-treatment with Rg3RGE (Fig. 3A), indicating that Rg3RGE-induced increase of cleaved PARP was not associated with initiation of autophagy. Next, Co-treatment with Rg3RGE and Chloroquine (CQ), which suppresses autophagic degradation by inhibiting lysosomal proteases, enhanced accumulation of LC3II and p62 relative to single-agent treatment in $CoCl_2$-stimulated breast cancer cells (Fig. 3B). Cleaved PARP levels were also modestly increased by co-treatment with Rg3RGE and CQ, suggesting that inhibition of lysosomal degradation in $CoCl_2$-stimulated autophagy promoted cell death. Furthermore, Spautin-1, which inhibits initiation of autophagy, inhibited the LC3II accumulation caused by Rg3RGE treatment and suppressed Rg3RGE-induced p62 and cleaved PARP in $CoCl_2$-stimulated cells (Fig. 3C). Furthermore, rapamycin and CQ did not significantly affect Rg3RGE-induced apoptosis. However, spautin-1 suppressed Rg3RGE-induced apoptosis in $CoCl_2$-stimulated breast cancer cells (Fig. 3D), indicating that Rg3RGE promoted apoptosis by inhibiting lysosomal degradation of autophagosomes in $CoCl_2$-induced autophagy.

3.4. Rg3RGE inhibits $CoCl_2$-stimulated autophagy by increasing ROS levels in breast cancer cells

HIF-1α stabilization plays a critical role in hypoxia-induced autophagy. Rg3RGE enhanced $CoCl_2$-induced HIF-1α stabilization in both breast cancer cell lines (Fig. 4A), indicating that Rg3RGE-inhibited autophagy was not related to HIF-1α stabilization. Rg3RGE significantly increased ROS levels, which modulate the HIF-1α stabilization and autophagy [22,23], in both the presence and absence of $CoCl_2$ (Fig. 4B). The ROS scavenger N-acetylcysteine (NAC) decreased Rg3RGE-induced ROS levels and HIF-1α stabilization (Fig. 4C), suggesting that Rg3RGE increased HIF-1α stabilization by increasing ROS levels in $CoCl_2$-stimulated cells. In addition, NAC decreased $CoCl_2$-induced spheroid formation and restored Rg3RGE reduction of spheroid size, resulting in sizes similar to spheroids under normoxic conditions (Fig. 4D). Rg3RGE-induced LC3 expression was also suppressed by NAC in $CoCl_2$-stimulated cells (Fig. 4E). Western blot results also showed that NAC significantly suppressed Rg3RGE enhancement of LC3II and P62 levels in $CoCl_2$-stimulated cells (Fig. 4F). Although ROS inhibition did not affect the lysosome activity, ROS inhibition suppressed accumulation of autophagosomes by inhibiting LC3 levels in cells treated with $CoCl_2$ and Rg3RGE (Fig. 4G). Together, these observations demonstrated that Rg3RGE suppressed $CoCl_2$-stimulated autolysosome formation by increasing oxidative stress.

3.5. Rg3RGE induces apoptosis by increasing ROS levels in breast cancer cells

Because Rg3RGE inhibited autophagy by increasing ROS levels, we hypothesized that Rg3RGE regulation of ROS levels was central to its the anti-tumor effects. As expected, ROS inhibition with NAC was protective against Rg3RGE decrease of cell viability and Rg3RGE-induced cell death (Fig. 5A and B). Further, Rg3RGE-induced increase of apoptotic markers was markedly inhibited by NAC in $CoCl_2$-stimulated breast cancer cells (Fig. 5C). Flow cytometry analysis revealed that NAC did not affect apoptosis in cells treated with $CoCl_2$ alone. However, apoptotic cells were significantly decreased in $CoCl_2$-stimulated breast cancer cells treated with Rg3RGE in combination with NAC than in $CoCl_2$-stimulated cells treated with Rg3RGE alone (Fig. 5D). Together, these results suggest that Rg3RGE induced apoptotic cell death by disrupting autophagy via increased intracellular ROS levels.

3.6. Rg3RGE induces apoptosis and suppresses autophagy in vivo

To determine if the anti-cancer effects of Rg3RGE were recapitulated *in vivo*, xenografts were generated in athymic nude mice by injection of MCF-7 cells into each flank. Tumor size significantly increased in the control group during the 21-day period. By contrast, tumor progression in mice treated with 50 mg/kg Rg3RGE was significantly slower than that of the control group (Fig. 6A). At the experimental endpoint of 21 days post-injection, tumor sizes, and tumor weights were smaller in the Rg3RGE group than in the control group (Fig. 6B and C). These results suggested that Rg3RGE decreased cancer progression *in vivo*. Consistent with *in vitro* findings, Rg3RGE significantly increased cleaved PARP and cleaved caspase 3 levels in xenografts (Fig. 6D). Rg3RGE treatment also increased p62 expression, as demonstrated by Western blot and IHC. Further, Rg3RGE dramatically decreased ki67 expression (proliferation maker) (Fig. 6E and F). Together, these findings suggested that Rg3RGE induced apoptosis and inhibited cell proliferation and autophagy *in vivo*.

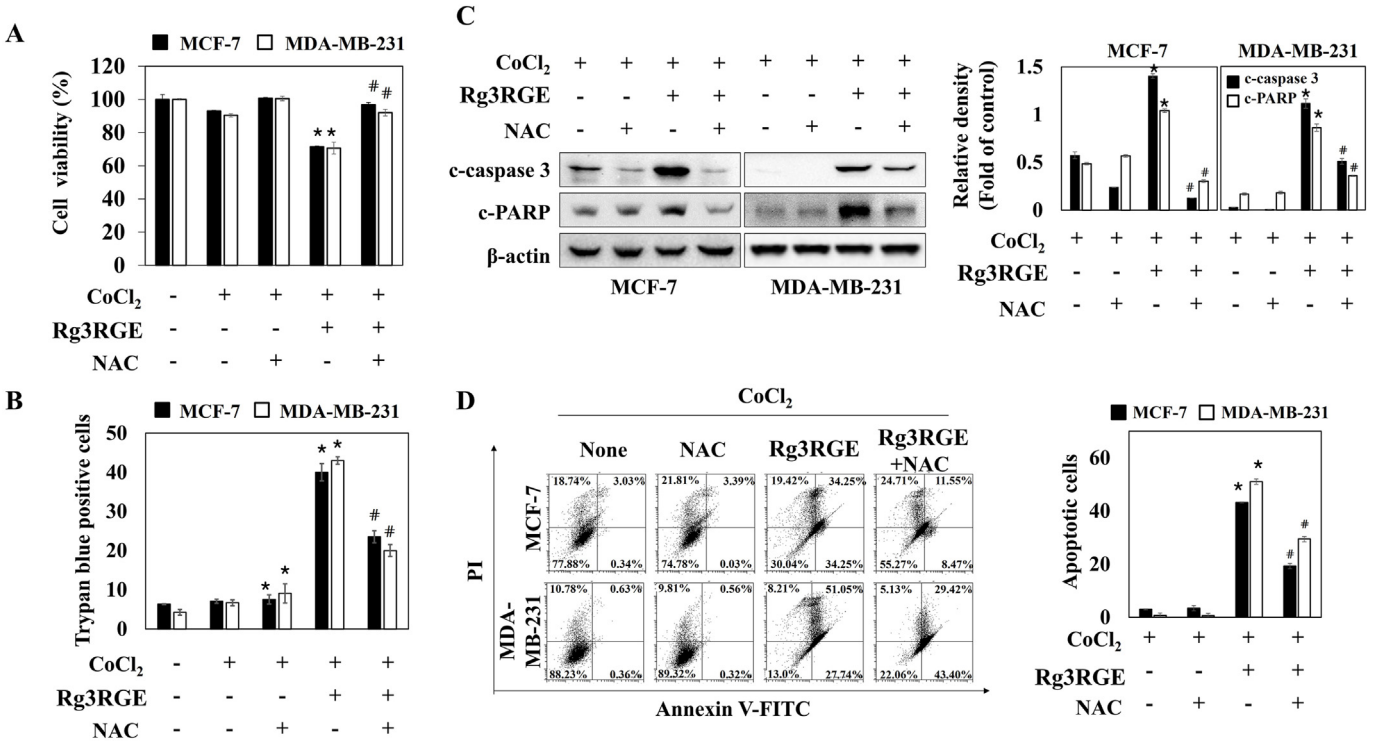

Fig. 5. Rg3RGE promotes apoptosis in breast cancer cells via induction of ROS. (A) MCF-7 and MDA-MB-231 cells were treated with 100 μM $CoCl_2$, 200 μg/ml Rg3RGE and 5 mM NAC for 24 h, followed by treatment with WST-1 solution for 2 h. (B) The number of trypan blue stained cells were analyzed. (C) After cells were treated with $CoCl_2$, Rg3RGE, and NAC for 24 h, levels of cleaved cspase3 and cleaved PARP were determined. β-actin was used as a loading control. The protein levels were quantified using ImageJ. (D) Rates of apoptosis were detected by flow cytometry. Results represent mean ± S.E.M. of three independent experiments. $^{*}P < 0.05$ vs. control. $^{\#}P < 0.05$ vs. Rg3RGE.

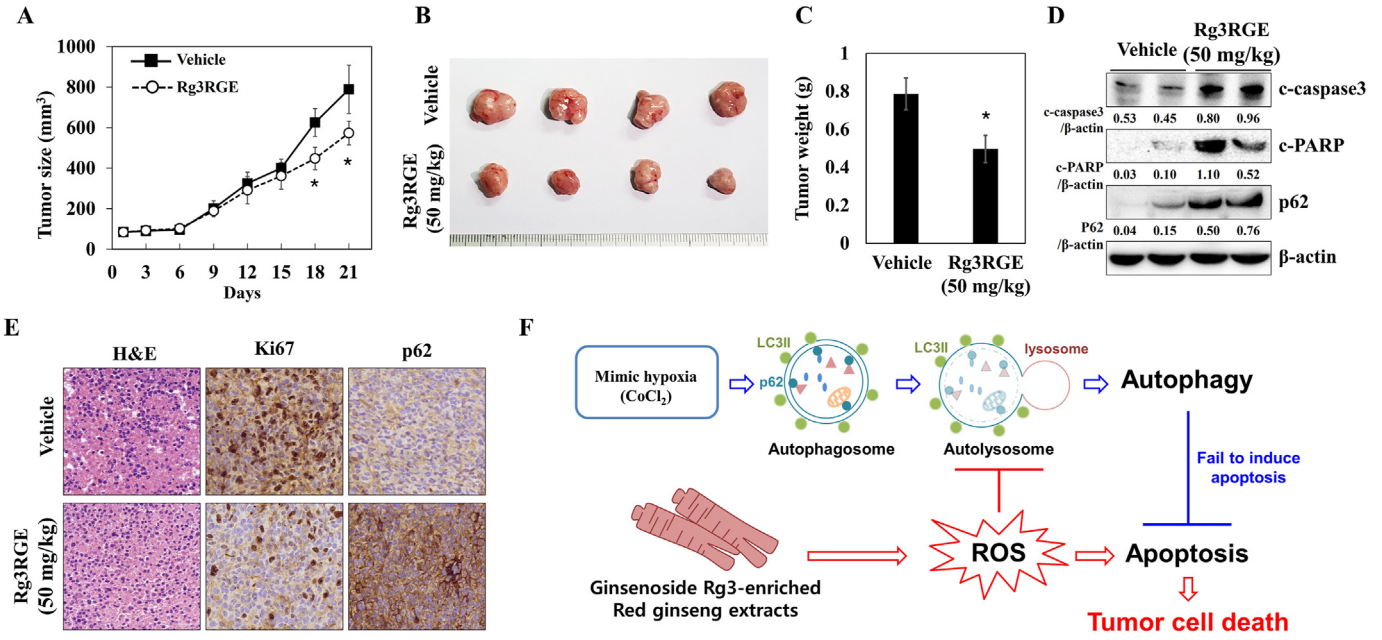

Fig. 6. Rg3RGE inhibits tumor growth *in vivo*. (A) MCF-7 cells (2×10^7 cells/mouse) were injected into the right flank of BALB/c nude mice. Results represent mean ± S.E.M. *$p \leq 0.05$ compared to vehicle group. Control vehicle group was treated with PBS containing 0.05% (v/v) Tween 20 (100 μl), and an Rg3RGE group was treated with 50 mg/kg/100 μl Rg3RGE. Tumor growth was monitored for 21 days (B) After 21 days of treatment, tumors were removed and photographed. (C) Tumor weights were determined (mean ± SE). *$p \leq 0.05$ compared to vehicle group. (D) The levels of cleaved caspase 3, cleaved PARP, and p62 in tumor tissues determined by Western blot analysis. The protein levels were quantified using ImageJ. (E) Tumor tissue confirmation by examination of H&E-stained sections under a dissecting microscope. The tumor tissues were immunostained using anti-Ki67 and p62 antibodies. (F) Model of the effect of Rg3RGE-induced ROS levels on apoptosis by inhibition of autolysosome formation in $CoCl_2$-stimulated breast cancer cells.

4. Discussion

Hypoxia is a primary feature of solid tumors, which develop resistance to chemotherapy by adapting to hypoxic conditions [24]. Korean red ginseng extract (RGE) and its bioactive components, including Rg3, affect HIF-1α stabilization in multiple cell lines under hypoxic conditions. RGE disrupts dimerization of HIF-1α and ARNT [25], while low-dose Rg3 induces HIF-1α activation under hypoxic conditions in liver cancer cells [26]. In addition, RGE suppresses cell migration by impairing hypoxia-induced EMT in colon cancer cells [27]. However, prior to the present study, the anticancer effects of RGE and Rg3 in hypoxia-stimulated breast cancer cells had not been investigated.

In this study, we demonstrated for the first time that Rg3RGE induces apoptosis of breast cancer cells treated with $CoCl_2$, which mimics hypoxia, by inhibiting autophagy. Generally, autophagy is considered to be a cell survival mechanism that confers resistance to cytotoxicity and combat hypoxic stress in the tumor microenvironment [28]. We demonstrated that $CoCl_2$-stimulated hypoxic stress increased autophagy in breast cancer cells. Rg3RGE accumulated LC3II expression and prevented autolysosome formation by suppressing expression of TFEB, a factor involved in lysosome activity, thereby disrupting autophagy and inducing apoptosis. Spautin-1 suppressed initiation of autophagy, but did not promote apoptosis in hypoxia-like conditions. Collectively, these findings suggest that induction of autophagy alone did not cause apoptosis in hypoxia. Interestingly, Chloroquine, which inhibits autophagosome-lysosome fusion, induced apoptosis in hypoxic breast cancer cell lines, similarly to Rg3RGE. Thus, autophagosome accumulation is a potential means to suppress cell survival mechanisms in hypoxic stress.

Intracellular ROS levels modulate autophagy by multiple mechanisms. To protect against ROS-induced mitochondrial damage, mitophagy increases in hypoxia-stimulated cells. Conversely, ROS inhibit autophagy via oxidation of ATG proteins and inactivation of TFEB [29,30]. This is consistent with our finding that Rg3RGE suppresses autophagosome-lysosome fusion by increasing ROS levels and subsequently inhibiting TFEB expression. Further, increased ROS levels inhibit proliferation and activate apoptosis by damaging cellular proteins, lipids, and DNA [31]. Accordingly, ROS inhibition prevented Rg3RGE-stimulated apoptosis and Rg3RGE inhibition of autophagy. Therefore, we suggest that ROS production is a key factor in Rg3RGE-modulated cell death.

In the present study, we demonstrated that Rg3RGE-stimulated ROS production mediates not only autophagy disruption, but also induction of apoptosis under hypoxia-like conditions (Fig. 6F). In addition, accumulation of autophagosomes plays an essential role in the apoptotic effects of Rg3RGE. *In vivo* studies also demonstrate that Rg3RGE inhibits breast cancer cell growth *in vivo* and increases protein levels of p62, an indicator of autophagosome accumulation. Based on these findings, we not only suggest that Rg3RGE is a putative breast cancer therapeutic modality, but also propose that promoting autophagosome accumulation is a potential novel therapeutic strategy for breast cancer treatment.

Declaration of competing interest

The authors have no conflicting interests.

Acknowledgments

This research was supported by the Korean Society of Ginseng (2021) and National Research Foundation of Korea (NRF) grants funded by the Korean government (MSIT) (2022R1A4A5032702)

Appendix A. Supplementary data

Supplementary data to this article can be found online at https://doi.org/10.1016/j.jgr.2023.06.001.

References

[1] Torre LA, Islami F, Siegel RL, Ward EM, Jemal A. Global cancer in women: burden and trends. Cancer Epidemiol Biomarkers Prev 2017;26(4):444–57.
[2] Moo TA, Sanford R, Dang C, Morrow M. Overview of breast cancer therapy. PET Clin 2018;13(3):339–54.
[3] Paraskevi T. Quality of life outcomes in patients with breast cancer. Oncol Rev 2012;6(1):e2.
[4] Elmore S. Apoptosis: a review of programmed cell death. Toxicol Pathol 2007;35(4):495–516.
[5] Bursch W, Ellinger A, Gerner C, Frohwein U, Schulte-Hermann R. Programmed cell death (PCD). Apoptosis, autophagic PCD, or others? Ann N Y Acad Sci 2000;926:1–12.
[6] Su M, Mei Y, Sinha S. Role of the crosstalk between autophagy and apoptosis in cancer. J Oncol 2013;2013:102735.
[7] Pan H, Wang Y, Na K, Wang Y, Wang L, Li Z, et al. Autophagic flux disruption contributes to Ganoderma lucidum polysaccharide-induced apoptosis in human colorectal cancer cells via MAPK/ERK activation. Cell Death Dis 2019;10(6):456.
[8] Su Z, Yang Z, Xu Y, Chen Y, Yu Q. Apoptosis, autophagy, necroptosis, and cancer metastasis. Mol Cancer 2015;14:48.
[9] Zaarour RF, Azakir B, Hajam EY, Nawafleh H, Zeinelabdin NA, Engelsen AST, et al. Role of hypoxia-mediated autophagy in tumor cell death and survival. Cancers (Basel). 2021;13(3).
[10] Lee JI, Park KS, Cho IH. Panax ginseng: a candidate herbal medicine for autoimmune disease. J Ginseng Res 2019;43(3):342–8.
[11] Kim JH. Pharmacological and medical applications of Panax ginseng and ginsenosides: a review for use in cardiovascular diseases. J Ginseng Res 2018;42(3):264–9.
[12] Zou M, Wang J, Gao J, Han H, Fang Y. Phosphoproteomic analysis of the antitumor effects of ginsenoside Rg3 in human breast cancer cells. Oncol Lett 2018;15(3):2889–98.
[13] Hwang SK, Jeong YJ, Cho HJ, Park YY, Song KH, Chang YC. Rg3-enriched red ginseng extract promotes lung cancer cell apoptosis and mitophagy by ROS production. J Ginseng Res 2022;46(1):138–46.
[14] Kim BM, Kim DH, Park JH, Surh YJ, Na HK. Ginsenoside Rg3 inhibits constitutive activation of NF-kappaB signaling in human breast cancer (MDA-MB-231) cells: ERK and akt as potential upstream targets. J Cancer Prev 2014;19(1):23–30.
[15] Peng Y, Zhang R, Yang X, Zhang Z, Kang N, Bao L, et al. Ginsenoside Rg3 suppresses the proliferation of prostate cancer cell line PC3 through ROS-induced cell cycle arrest. Oncol Lett 2019;17(1):1139–45.
[16] Shan K, Deng Y, Du Z, Yue P, Yang S. Examination of combined treatment of ginsenoside Rg3 and 5-fluorouracil in lung adenocarcinoma cells. Comput Math Methods Med 2022;2022:2813142.
[17] Bian S, Zhao Y, Li F, Lu S, Wang S, Bai X, et al. 20(S)-Ginsenoside Rg3 promotes HeLa cell apoptosis by regulating autophagy. Molecules 2019;24(20).
[18] Jeong D, Irfan M, Kim SD, Kim S, Oh JH, Park CK, et al. Ginsenoside Rg3-enriched red ginseng extract inhibits platelet activation and in vivo thrombus formation. J Ginseng Res 2017;41(4):548–55.
[19] Owada S, Ito K, Endo H, Shida Y, Okada C, Nezu T, et al. An adaptation system to avoid apoptosis via autophagy under hypoxic conditions in pancreatic cancer cells. Anticancer Res 2017;37(9):4927–34.
[20] Yoshii SR, Mizushima N. Monitoring and measuring autophagy. Int J Mol Sci 2017;18(9).
[21] Song W, Wang F, Savini M, Ake A, di Ronza A, Sardiello M, et al. TFEB regulates lysosomal proteostasis. Hum Mol Genet 2013;22(10):1994–2009.
[22] Jung SN, Yang WK, Kim J, Kim HS, Kim EJ, Yun H, et al. Reactive oxygen species stabilize hypoxia-inducible factor-1 alpha protein and stimulate transcriptional activity via AMP-activated protein kinase in DU145 human prostate cancer cells. Carcinogenesis 2008;29(4):713–21.
[23] Chang KC, Liu PF, Chang CH, Lin YC, Chen YJ, Shu CW. The interplay of autophagy and oxidative stress in the pathogenesis and therapy of retinal degenerative diseases. Cell Biosci 2022;12(1):1.
[24] Semenza GL. Defining the role of hypoxia-inducible factor 1 in cancer biology and therapeutics. Oncogene 2010;29(5):625–34.
[25] Choi YJ, Choi H, Cho CH, Park JW. Red ginseng deregulates hypoxia-induced genes by dissociating the HIF-1 dimer. J Nat Med 2011;65(2):344–52.
[26] Shi L, Pi Y, Luo C, Zhang C, Tan D, Meng X. In vitro inhibitory activities of six gypenosides on human liver cancer cell line HepG2 and possible role of HIF-1alpha pathway in them. Chem Biol Interact 2015;238:48–54.
[27] Kim EJ, Kwon KA, Lee YE, Kim JH, Kim SH, Kim JH. Korean Red Ginseng extract reduces hypoxia-induced epithelial-mesenchymal transition by repressing NF-kappaB and ERK1/2 pathways in colon cancer. J Ginseng Res 2018;42(3):288–97.
[28] Folkerts H, Hilgendorf S, Vellenga E, Bremer E, Wiersma VR. The multifaceted role of autophagy in cancer and the microenvironment. Med Res Rev 2019;39(2):517–60.
[29] Filomeni G, Desideri E, Cardaci S, Rotilio G, Ciriolo MR. Under the ROS…thiol network is the principal suspect for autophagy commitment. Autophagy 2010;6(7):999–1005.
[30] Su Q, Zheng B, Wang CY, Yang YZ, Luo WW, Ma SM, et al. Oxidative stress induces neuronal apoptosis through suppressing transcription factor EB phosphorylation at Ser467. Cell Physiol Biochem 2018;46(4):1536–54.
[31] Aggarwal V, Tuli HS, Varol A, Thakral F, Yerer MB, Sak K, et al. Role of reactive oxygen species in cancer progression: molecular mechanisms and recent advancements. Biomolecules 2019;9(11).